Experimental and Numerical Study of the Structural Stiffness of a Composite Rotor Blade

Hyeon-Kyu Jeon[1], Min-Hyeok Jeon[1], Min-Song Kang[1], In-Gul Kim[1]*, Jae-Sang Park[1], and Jin-Young Seok[1]

[1] Department of Aerospace Engineering, Chungnam National University, Daejeon, Republic of Korea

* Corresponding author (igkim@cnu.ac.kr)

ABSTRACT

The basic mechanical properties of helicopter rotor blade are important parameters when analyzing the helicopter performance of a helicopter. However, it is difficult to estimate these properties because most rotor blades consist of various materials, such as composite materials and metals. In this paper, the bending/torsional stiffness of a composite rotor blade of an unmanned helicopter are evaluated through experimental and analytical studies. In finite element analysis(FEA), the bending/torsional stiffness are evaluated through the relationship between the load-displacement and element stiffness matrix. The evaluated stiffness from the measured strains and displacements in bending and torsional test agreed well with the calculated results of FEA.

KEYWORDS: *Composite Rotor Blade, Cross-sectional Stiffness, Bending Test, Torsional Test, Stiffness Matrix*

1 INTRODUCTION

The helicopter rotor blade, which produces lift, thrust, and control force, is the major structure of the helicopter, having major effects on performance. However, it operates under the complex aerodynamic conditions, and certain problems can be arise, such as stability, fatigue, and vibration due to structural-aerodynamic coupling responses. Thus, when a new helicopter is designed, the structural and aerodynamic characteristics of the rotor blade to be used must be considered (Yun, 2015).

To analyze the helicopter performance, the rotor blade can be assumed as an elastic body. Hence, the basic properties of the mass distribution as well as certain mechanical characteristics, specifically the bending and torsional stiffness, are needed as parameters to be input into the analysis. As the results of such an analysis are influenced by the accuracy of these mechanical characteristics, correct evaluations of the mechanical characteristics are important. However, modern helicopter rotor blades consist of various materials, such as composite materials and different type of metal. Specifically, the bending/torsional stiffness can vary depending on the fiber and matrix materials and on the stacking sequences of the composites. Accordingly, experimental and numerical methods must be used in these evaluations.

To do this, Enei (2015) introduced a test method which calculates the cross-sectional properties through displacement information obtained by photogrammetric detection techniques and evaluated the mechanical characteristics of a composite rotor blade using this method. Hoffmann (2016) calculated the shear center and cross-sectional stiffness of a rotor blade by obtaining displacement and twist angle data from images for a non-rotating dynamic test of the rotor blade. Additionally, You (2011) calculated the cross-sectional stiffness of a box-shaped composite beam by means of a FEA for the optimal structural design of the turbine blade.

In this paper, bending and torsional test were conducted to evaluate the cross-sectional bending and torsional stiffness of a composite rotor blade. A FEA was performed with the modeled rotor blade and the equivalent stiffness of the rotor blade beam was calculated with the cross-sectional stiffness matrix.

2 TEST METHOD AND PROCEDURE

2.1 Test setup and methods

The object of study is the main rotor blade of an unmanned helicopter. As shown in Figure 1, the rotor blade consist of CFRP (Carbon Fabric Reinforced Plastic) and GFRP (Glass Fabric Reinforced Plastic), and these materials exist at different locations on the blade. The initial incidence angle is from the root to the tip.

To evaluate the cross-sectional stiffness, bending and torsional tests were performed. Figure 2 presents a schematic representation of the apparatus. The rotor blade was fixed with a fastener and plywood, and it was fixed at the beginning of the airfoil section using airfoil-shaped plywoods and steel jigs. Strain gauges were attached at different locations onto the rotor blade, and strain data was acquired with a multi-strain amp (MGC. Plus). Acrylic jigs were attached onto the lower surface of the rotor blade to measure the displacement due to the load with the laser sensors (L-LAS-LT-30-SL-P).

The devices used to apply the load to the rotor blade for the bending and torsional tests are presented in Figure 3. The device used in the bending test has a rod attached to a load cell to measure reaction forces due to deformation and to produce displacement on the rotor blade. The device for the torsional test consists of a pulley and weights to apply torsional loads to the leading/trailing edge of the rotor blade.

A schematic of the bending and torsional test conducted to evaluate the cross-sectional stiffness is presented in Figure 4. Prior to the bending and torsional tests, the cross-sectional shear center was estimated to minimize the coupling of the bending-torsional deformation. The bending test was performed by applying loads at the estimated average position of the shear center, and the bending stiffness (EI) was evaluated from the relationship between the measured loads, the strain, and the displacement. The torsional test was performed by applying torsional loads at the tip of the rotor blade and the torsional stiffness (GJ) was evaluated by assessing the relationship between the torsional load and the shear strain.

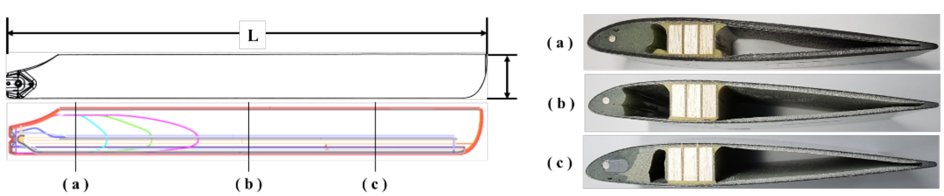

Figure 1: Rotor blade specimen

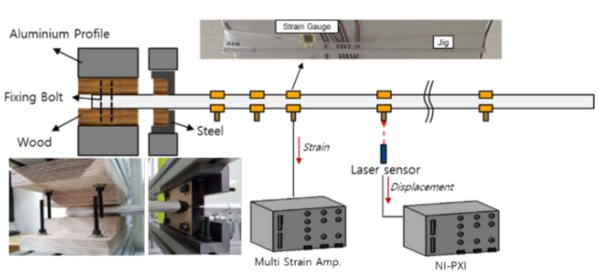

Figure 2 : Schematic representation of the test apparatus

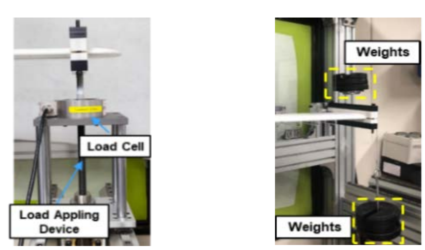

(a) Device for bending test (b) Device for torsional test

Figure 3 : Device used to apply loads

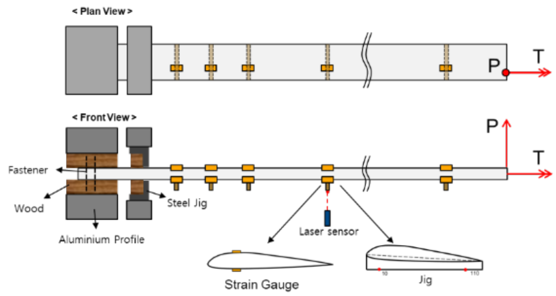

Figure 4 : Schematic representation of the bending/torsional test

2.2 Estimating the Shear Center during the Test

With regard to the test and FEA, estimating the shear center of each section should be done beforehand to minimize the coupled bending-torsional deformation. Because the shear center in the cross-section is the point at which bending and torsional deformation occurs independently, torsional deformation occurs with respect to the shear center. In this paper, as shown in Figure 5, the intersection point at which deformation occurs for different torsional loads within the section was estimated as the shear center of each section.

Two conditions (pitch-up/down) of the torsional load were applied at the tip of the rotor blade to estimate the shear center of each section. The twist of rotor blade was determined from the vertical displacement as measured with laser sensors. The result of estimating the shear center is shown in Figure 6.

2.3 Bending/Torsional Test

The bending stiffness (EI) of the rotor blade was evaluated through a bending test. To evaluate the bending stiffness, strain gauges were attached to the upper and lower surfaces at eleven points on the rotor blade, as shown in Figure 7. The displacements of the leading edge and the trailing edge due to the bending load were also measured with the laser sensors. The bending load was applied as a concentrated load to the average chordwise position of the estimated shear center at the tip of the rotor blade. This type of load was applied to make the displacement at the tip of the rotor blade have 5%, 7.5%, and 10% of span.

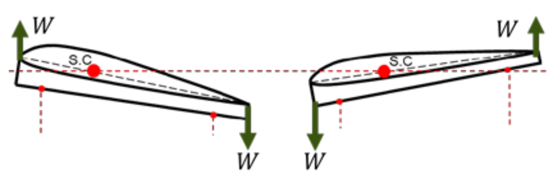

Figure 5 : Schematic representation of a twisted cross-section under different load cases

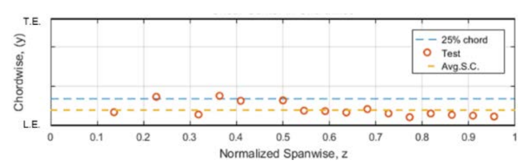

Figure 6 : Estimated and average positions of the shear center

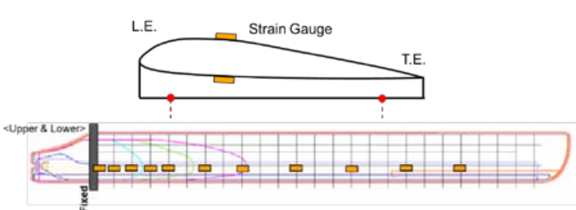

Figure 7 : Strain gauges installed for the bending test

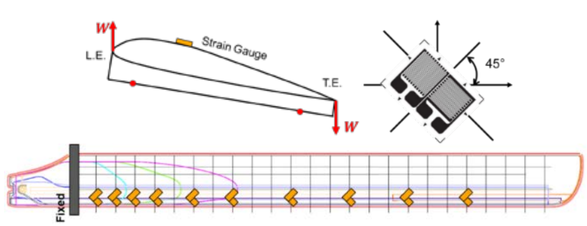

Figure 8 : Strain gauges installed for the torsional test

2.4 Torsional Test

The torsional test to evaluate the torsional stiffness (GJ) was conducted by applying a pitch-up torsional load in the form of a coupled load at the leading edge and trailing edge of the tip of the rotor blade (Berring, 2007), as shown in Figure 8. The shear strain due to the torsional load was calculated with a normal strain gauge attached in ±45° directions.

3 NUMERICAL ANALYSIS

3.1 Finite Element Model

In order to calculate the shear center and stiffness of the rotor blade, a linear static analysis (SOL 101) was conducted with the commercial finite element analysis program: MSC. NASTRAN / PATRAN. Referring to the sectional shape identified by a cross-section inspection of the produced rotor blades, the finite element model was devised using 2-D shell elements (CQUAD4) for the skins and 3-D solid elements (CHEX8) for spar and adhesive components. The properties applied to the skin of the finite element model were entered into several divided areas, taking into account the composite stacks applied to the rotor blades, as shown in Figure 9. The boundary condition was applied as a fixed condition to the root of the rotor blade.

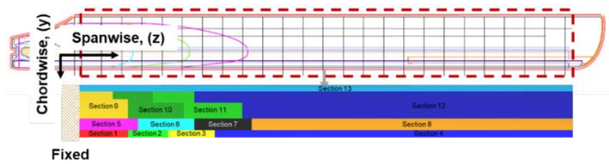

Figure 9 : Finite element model for the rotor blade

3.2 Estimating Shear Center in FEA

The shear center in a cross-section of the rotor blade can be estimated by means of a the geometric method as shown in Figure 10 (Houbolt, 1957). An arbitrary point (*f*) in the cross-section can be represented with the coordinate(x_i, y_i) using the relative distance with respect to the shear center. The coordinate$(x_i{}', y_i{}')$ after deformation due to an arbitrary load can be determined using as Eqs. (1) with the displacement(u, v) of the shear center, the displacement(u_i, v_i) of point (*f*), and the twist angle(ϕ).

$$\begin{cases} x_i' - x_i = u - y_i\phi = u_i \\ y_i' - y_i = -v + x_i\phi = v_i \end{cases} \tag{1}$$

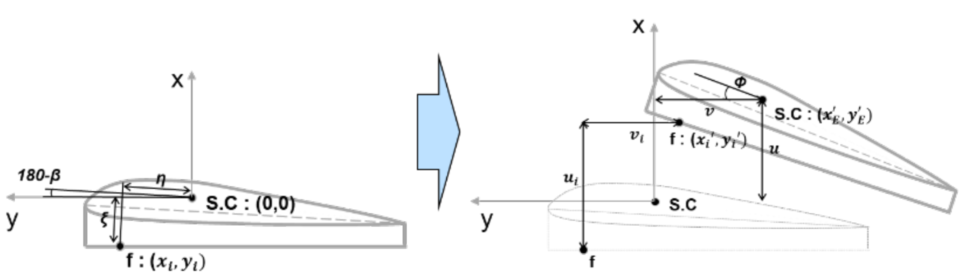

Figure 10 : Schematic representation for estimating shear center

The position of the shear center can be calculated with displacement and twist angle of point (*f*) in Eqs. (1) for each load case. The result of the estimated shear center of the rotor blade calculated from the

FEA is presented in Figure 11. It was found that the chordwise shear centers are located 20% $\bar{c}$ ahead of quarter chord (1/4 $\bar{c}$), while the flapwise shear centers are located at 11 % of the thickness from above the mid-line of the rotor blade.

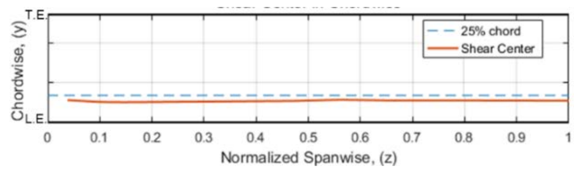

(a) Shear center chordwise

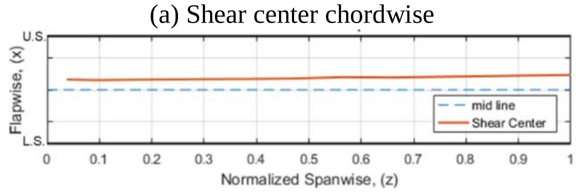

(b) Shear center flapwise

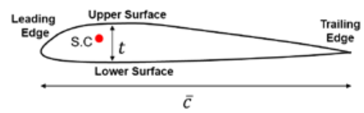

Figure 11 : The position of the shear center in the (a) chordwise, and (b) flapwise directions

3.3 Sectional Stiffness Matrix

It is possible to calculate the sectional stiffness using the displacement of each node from the FEA. Eqs. (2) can be derived from a combination of Eqs. (3) and Eqs. (4). Eqs. (3) represents the load-displacement relationship pertaining to six load conditions ($F_x, F_y, F_z, M_x, M_y, M_z$) acting on the tip of the blade as shown in Figure 12. Eqs. (4) represents the internal force-relative displacement of the elements. Eqs. (2) is in the form of the Lyapunov equation, with this equation, it is possible to calculate the stiffness at each section by solving it respect to the sectional stiffness matrix, *k*. The bending/torsional stiffness calculated with the sectional stiffness matrix is presented in Figure 13.

$$\mathrm{K}^{-1}Q^{-1} = k^{-1}HQ + Ek^{-1} \tag{2}$$

$$\{u^{rl}\} = [K^{-1}]\{f^{r}\} \tag{3}$$

$$\{\mathrm{u}^{\mathrm{rl}}\} = (k^{-1}\mathrm{H} + \mathrm{E}k^{-1}Q)f^{r} \tag{4}$$

$$\mathrm{k} = \begin{bmatrix} GA_x & & & & & \\ & GA_y & & & & \\ & & EA & & & \\ & & & EI_x & & \\ & & & & EI_y & \\ & & & & & GJ \end{bmatrix} \tag{5}$$

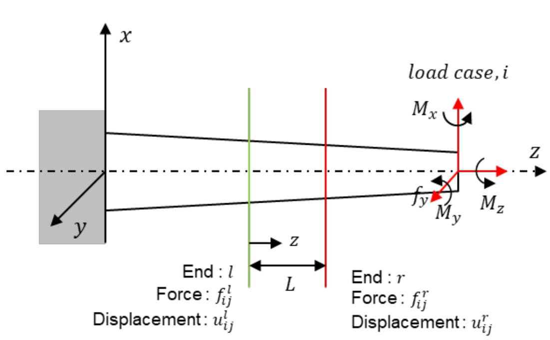

Figure 12 : Equivalent beam model of the rotor blade

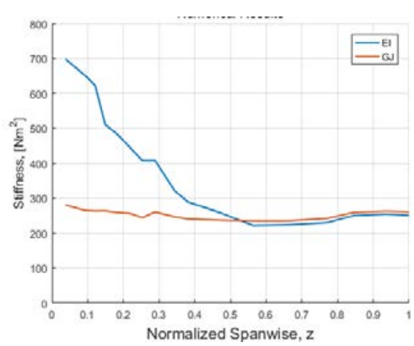

Figure 13 : Evaluated bending(EI)/torsional(GJ) stiffness

4 RESULTS AND DISCUSSION

4.1 Bending Stiffness

Figure 14 presents a comparison of the strain results of the test and FEA due to bending loads on the upper surface. The measured strain at the root in the test indicates that deformation occurred due to the incomplete realization of the fixed condition. Except for the root region, the strain results of the test are in good agreement with the results of the FEA.

Figure 15 presents a comparison of the bending stiffness as evaluated by the experimental and numerical methods. The bending stiffness from the test was evaluated using Eqs. (6) with the applied moment M, the distance between gauges (as shown in Figure 16) h, and the measured strain ε. In all load cases, the results of the bending stiffness were calculated equivalently. These showed good agreement with the numerical result using the sectional stiffness matrix.

$$EI_i = \frac{Mh}{|\varepsilon_{upper}| + |\varepsilon_{lower}|} \tag{6}$$

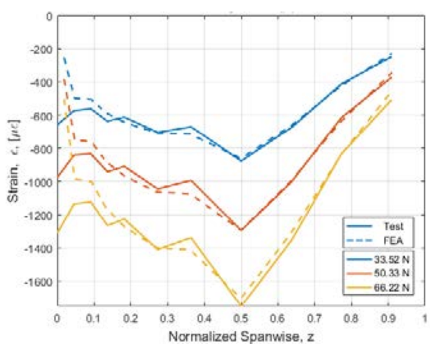

Figure 14 : Comparison of the strain results from the test and FEA

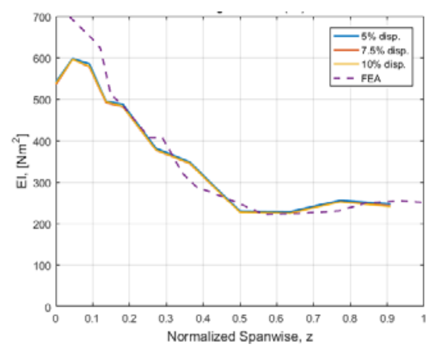

Figure 15 : Comparison of the bending stiffness from the experimental and numerical results

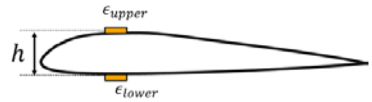

Figure 16 : Distance between the strain gauges

4.2 Torsional Stiffness

Figure 17 presents a comparison of the shear strain results of the test and the FEA when applying a torsional load. Similar to the bending case, the strain results of the test were in good agreement with the results of the FEA, except for the root region.

Figure 18 presents a comparison of the torsional stiffness as evaluated by the experimental and numerical methods. The torsional stiffness from the test was evaluated with Eqs. (7) with the applied torque T, the shear strain γ, and the normal distance from the shear center to the point at which the strain measured r (as shown in Figure 19). In all load cases, except for the root region, where the strain is complex, the results of torsional stiffness were calculated equivalently and these results were in good agreement with the numerical result using the sectional stiffness matrix.

$$GJ_i = \frac{Tr}{\gamma} \tag{7}$$

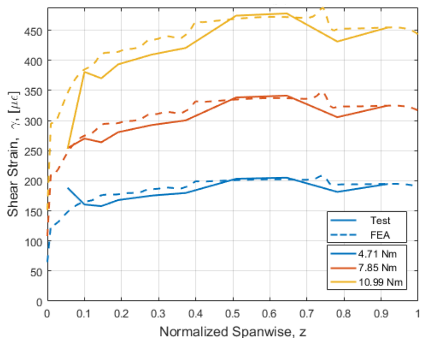

Figure 17 : Comparison of the shear strain results from the test and the FEA

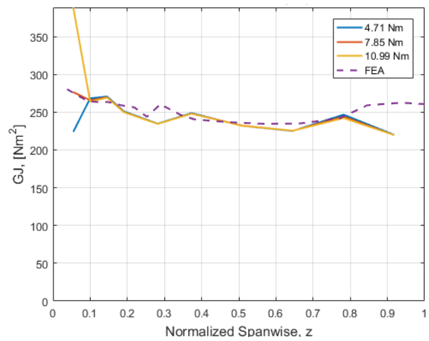

Figure 18 : Comparison of the torsional stiffness from the experimental and numerical results

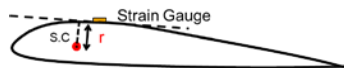

Figure 19 : Normal distance to the shear center in the cross-section

5 CONCLUSION

In this paper, the shear center and cross-sectional stiffness were evaluated with experimental and numerical methods. In order to minimize any coupled bending-torsional deformation, the shear center was estimated first. Subsequently, the cross-sectional bending and torsional stiffness were evaluated from bending and torsional tests. Furthermore, through a FEA, the shear center was estimated with a geometric method, and using a cross-sectional stiffness matrix, the bending and torsional stiffness were calculated.

The numerical results for the bending/torsional stiffness were validated through a comparison of the results of the tests. Based on the verified results, it was possible to use the values of the sectional stiffness matrix to replace the values of the chordwise bending stiffness EI_x, the chordwise shear stiffness GA_y, the flapwise shear stiffness GA_x, and the spanwise extensional stiffness, EA which are difficult to evaluate experimentally.

From this study, it is shown to be possible to evaluate the shear center and cross-sectional stiffness of a rotor blade. These results are expected to be useful to those who analyze helicopter performance considering an elastic rotor blade and can likely be applied during the development of new composite rotor blades as well.

6 ACKNOWLEDGEMENTS

This research was supported by the Institute of Civil Military Technology Cooperation (ICMTC), Republic of Korea.

REFERENCES

Yun, C.Y. and Kim, D.K. (2015). The Measurement Test of Stiffness and Natural Frequencies for Bearingless Rotor System of Helicopter. *Transactions of the Korean Society for Noise and Vibration Engineering, 25(12)*, pp.881-887.

Enei, C., et al. (2015). Photogrammetric detection technique for rotor blades structural characterization. *Journal of Physics: Conference Series*, *658*(1), 012003.

Hoffmann, F., Keimer R. and Riemenschneider, J. (2016). Structural Modeling and Validation of an Active Twist Model Rotor Blade. *CEIAS Aeronautical Journal*, 7(1), pp.43-55.

You, G.S. (2011). *An Optimal Structural Design of Composite Box Structure using Equivalent Cross-section Characteristics.* Master's Thesis, Chungnam National University, Republic of Korea.

Berring, P., Branner, K., Berggreen, C. and Knudsen, H.W. (2007). Torsional Performance of wind turbine blades – Part 1: Experimental Investigation. *Proceeding of 16th International Conference on Composite Materials (Vol.43). Japan Society for Composite Materials.*

Houbolt, J.C. and George, W.B. (1957). Differential Equations of Motion for Combined Flapwise Bending, Chordwise, Bending and Torsion of Twisted Nonuniform Rotor Blade (NACA Technical Note 3905).